# Velocity shear generated Alfvén waves in electron-positron plasmas

Andria D. Rogava

*Department of Theoretical Astrophysics, Abastumani Astrophysical Observatory*

*Tbilisi, Republic of Georgia*

and

*International Centre for Theoretical Physics, Trieste, Italy*

S.M. Mahajan

*Institute for Fusion Studies, The University of Texas at Austin*

*Austin, Texas 78712*

and

*International Centre for Theoretical Physics, Trieste, Italy*

and

Vazha I. Berezhiani

*Department of Plasma Physics, Institute of Physics*

*The Georgian Academy of Science, Tbilisi 380077, The Republic of Georgia*

and

*International Centre for Theoretical Physics, Trieste, Italy*

**Abstract**

Linear magnetohydrodynamics (MHD) modes in a cold, nonrelativistic electron-positron plasma shear flow are considered. The general set of differential equations, describing the evolution of perturbations in the framework of the nonmodal approach is derived. It is found, that under certain circumstances, the compressional and shear Alfvén perturbations may exhibit large transient growth fuelled by the mean kinetic energy of the shear flow. The velocity shear also induces mode coupling allowing the

PACS No.: 52.30.-q, 52.35.Bj, 94.30.Tz, 97.60.Gb

exchange of energy as well as the possibility of a strong mutual transformation of these modes into each other. The compressional Alfvén mode may extract the energy of the mean flow and transfer it to the shear Alfvén mode via this coupling. The relevance of these new physical effects to provide a better understanding of the laboratory $e^+e^-$ plasmas is emphasized. It is speculated that the shear-induced effects in the electron-positron plasmas could also help solve some astrophysical puzzles (e.g., the generation of pulsar radio emission). Since most astrophysical plasmas are relativistic, it is shown that the major results of the study remain valid for weakly sheared relativistic plasmas.

# 1 Introduction

It is commonly recognized that electron-positron (henceforth referred as $e^+e^-$) plasmas are created in a variety of astrophysical situations. A well-known example is the pulsar magnetosphere, where in the super strong magnetic fields $B \sim 10^8 T$ $(10^{12} G)$, gamma rays, with energy greater than twice the rest energy of the electron, decay into $(e^+e^-)$ pairs: $\gamma + B \rightarrow e^- + e^+ + B$. The components of these (*primary*) pairs are accelerated to very high energies by parallel electric fields, and emit gamma rays, triggering, in turn, a *pair cascade*.[1] As a result of this process a *secondary* pair plasma with the mean Lorentz factor $\Gamma \sim 10^2 - 10^3$ and the multiplicity factor (the ratio of the number of secondaries to the number of primaries) $\mathcal{M} \sim 10^3 - 10^5$ is formed.[2]

The $e^+e^-$ plasmas are also likely to be found in the bipolar outflows (jets) in Active Galactic Nuclei (AGN),[3] and at the center of our own Galaxy.[4] In AGN's, the observations of superluminal motion are commonly attributed to the expansion of $e^+e^-$ relativistic beams pervading a subrelativistic medium. This model implies a copious production of $e^+e^-$ pairs via $\gamma - \gamma$ interactions creating an $e^+e^-$ atmosphere around the source. The actual production of $e^+e^-$ pairs due to photon-photon interactions happens in the coronae of AGN accretion discs, which upscatter the soft photons emitted by the accretion discs by inverse Compton

scattering.

The presence of $e^+e^-$ plasma is also argued in the MeV epoch of the early Universe.[5] In the standard cosmological model, temperatures in the MeV range ($T \sim 10^{10}K \sim 1\,\mathrm{MeV}$) prevail up to times $t \simeq 1$ sec after the Big Bang. In this epoch, the main constituent of the Universe is an $e^+e^-$ plasma in equilibrium with photons, neutrinos, anti-neutrinos and a minority population of heavier ions.

Contemporary progress in the production of pure positron plasmas[6] has also made it possible to create *nonrelativistic* $e^+e^-$ plasmas in the laboratory by a number of different experimental approaches (see Refs. 7 and 8 and references therein). The condition for the plasma collective effects to be important is that the annihilation (e.g., via positronium atom formation, or two-body collisions) time scale $t_a$ should be much longer than the time scale for plasma effects ($t_p \sim 1/\omega_p$). When this criterion ($t_a \gg t_p$) holds, experimental observation of the collective phenomena becomes possible.[8]

From the theoretical point of view the $e^+e^-$ plasma, being a subclass of equal-mass plasmas, may display physical processes and properties quite different from those of a conventional ion-electron plasma. In the latter case, the smallness of the $m_e/m_i$ ratio is exploited to an extensive degree and is responsible for certain well-known properties of such media. While in the former case, with equal absolute charge to mass ratio for both of the constituents, important symmetries should appear; these can lead to considerable simplification in the mathematical description of the collective phenomena in a $e^+e^-$ plasma.[8] Several novel features can also emerge.

During the last few years a considerable amount of work has been done in the analysis of linear and nonlinear Alfvén wave propagation in $e^+e^-$ plasmas. It is contended that these weakly damped waves (in contrast to e.g., Langmuir or magnetoacoustic waves) may be the source of the observed electromagnetic emission from the pulsars and the $e^+e^-$ jets. According to Mikhailovsky *et al.*,[9] among all the possible low-frequency modes in $e^+e^-$

plasma, the Alfvén waves are the most likely candidate to escape the pulsar magnetosphere.

Several linear and nonlinear processes have been proposed for the generation of Alfvén waves in an $e^+e^-$ plasma. For instance, a *linear* effect, which can lead to the excitation of Alfvén waves, is the Cherenkov interaction with plasma particles. However, this process requires an inversion in the distribution function, and, could not quite explain high levels of the observed radiation.[10] Further search for universal amplification effects, which can transfer the energy stored in an $e^+e^-$ plasma into Alfvén wave energy, therefore, is of principal importance in this context.

The aim of this paper is precisely to look for such a mechanism. We consider the problem of linear excitation, and the subsequent evolution of the Alfvén waves in a $e^+e^-$ plasma flow with *velocity shear*. Note that the shear flow possesses a considerable amount of kinetic energy, and that the associated velocity vector field is spatially inhomogeneous. The resulting velocity gradients may play quite unexpected and sometimes even crucial role in the overall dynamics of wave processes occurring in such flows. This conjecture was soundly confirmed recently; the use of an effective *nonmodal approach* to the study of physical processes in shear flows[11] reveals a whole branch of new physical phenomena provoked by the velocity shear in various kinds of hydrodynamic and hydromagnetic flows.[11–15] A particularly interesting example is the discovery of a new energy exchange mechanism between the mean flow and sound-type perturbations in a two-dimensional (2-D) compressible, plane Couette flow.[12] It was shown that the perturbations, *extracting* energy from the mean shear flow, may grow linearly in time.

Another new effect—the *linear* coupling and mutual transformation of waves with a corresponding energy transfer induced by the velocity shear—was found in Ref. 13. Originally, the effect was demonstrated for the simplest example, i.e., of the 2-D waves in an unbounded, parallel *hydromagnetic* flow with uniform velocity shear. It was subsequently shown that an analogous mechanism is operative in other kinds of parallel shear flows as long as the system

can naturally sustain several (more than one) modes.[14,15]

In this paper we explore the possibility of these effects in the shear flow of a magnetized, cold nonrelativistic $e^+e^-$ plasma. It is natural to expect that the shear induced effects will lead to interesting consequences for these flows. Qualitatively similar behavior should pertain for warm/hot and relativistic flows.

Before giving the plan of the paper, we would like to place this work in perspective. Since the typical transient phenomena induced by the velocity shear in different systems are rather similar in character, there is no new "fundamental" physics unearthed in this paper. The novelty, however, lies in: 1) the choice of a system which is of great astrophysical and cosmological significance, and 2) studying the interaction of the shear and compression Alfvén waves in a three dimensional flow, an investigation which could possibly help us in understanding the nature of the pulsar radiation. Towards this end, a more realistic relativistic theory is being developed. The two fluid model used in this paper further allows us to investigate mode-coupling mediated by the finite skin-depth effects, a process not available in MHD.

The paper is organized in the following way: In Sec. II, we present the general formalism: a universal set of linearized equations, describing the evolution of perturbations in a cold nonrelativistic sheared $e^+e^-$ plasma flow, are derived. (The detailed derivation of the *induction equation* is presented separately in Appendix A). In Sec. III, a model flow, with uniform shear, is investigated in considerable detail. Extremely interesting phenomena like the large transient amplifications of the Alfvén waves, and energy exchange between the 'shear' and the compressional Alfvén waves are appropriately demonstrated. The final section is devoted to a discussion of the possible applications of this new physics to the theory of pulsar radio emission, to the $e^+e^-$ jet outflows in AGN's, and related subjects.

Since most astrophysical flows tend to be relativistic, it is shown in Appendix B that the mathematical structure, and hence the basic physical results of the nonrelativistic approach,

remain essentially unchanged for a weakly-sheared relativistic flow.

## 2 General Formalism

The basic set of two-fluid magnetohydrodynamics (MHD) equations for the $e^+e^-$ plasma consists of the mass and momentum conservation equations, supplemented by Maxwell's equations:

$$\partial_t n^\pm + \nabla \cdot \left( n^\pm \mathbf{V}^\pm \right) = 0, \tag{1}$$

$$m n^\pm \left[ \partial_t + (\mathbf{V}^\pm, \nabla) \right] \mathbf{V}^\pm = \pm e n^\pm \left( \mathbf{E} + \frac{1}{c} \mathbf{V}^\pm \times \overline{\mathbf{B}} \right) - \nabla P^\pm, \tag{2}$$

$$\nabla \cdot \mathbf{E} = 4\pi e (n^+ - n^-), \tag{3}$$

$$\nabla \times \mathbf{E} = -\frac{1}{c} \partial_t \overline{\mathbf{B}}, \tag{4}$$

$$\nabla \cdot \overline{\mathbf{B}} = 0, \tag{5}$$

$$\nabla \times \overline{\mathbf{B}} = \frac{4\pi}{c} \mathbf{J} + \frac{1}{c} \partial_t \mathbf{E}, \tag{6}$$

where $\mathbf{J}$ is the current density vector

$$\mathbf{J} \equiv e(n^+ \mathbf{V}^+ - n^- \mathbf{V}^-), \tag{7}$$

and $n^\pm$, $\mathbf{V}^\pm$, and $P^\pm$ are respectively the number density, velocity and pressure of the appropriate species.

Let us consider an $e^+e^-$ plasma embedded in an external uniform magnetic field $\mathbf{B}_0 = (B_0,\ 0,\ 0)$ along the $x$-axis. The plasma is characterized by a sheared bulk flow velocity $\mathbf{U}_0$. The instantaneous values of velocity components for each species in the plasma may be decomposed into their mean and perturbed components:

$$\mathbf{V}^\pm \equiv \mathbf{U}_0^\pm + \mathbf{u}^\pm = \mathbf{U}_0 + \mathbf{u}^\pm. \tag{8}$$

Similarly writing $\overline{\mathbf{B}} = \mathbf{B}_0 + \mathbf{B}$, we can derive the linearized versions of (1)–(6). Equations (3)–(5) remain the same, while the rest take the form:

$$D_t n^{\pm} + n_0 \nabla \cdot \mathbf{u}^{\pm} = 0, \tag{9}$$

$$D_t \mathbf{u}^{\pm} + (\mathbf{u}^{\pm}, \nabla)\mathbf{U}_0 = -\left(\frac{C_s^2}{n_0}\right)\nabla n^{\pm} \pm \frac{e}{m}\left(\mathbf{E} + \frac{\mathbf{U}_0}{c} \times \mathbf{B} + \frac{\mathbf{u}^{\pm}}{c} \times \mathbf{B}_0\right), \tag{10}$$

$$\nabla \times \mathbf{B} = \frac{4\pi e}{c}\left[(n_+ - n_-)\mathbf{U}_0 + n_0(\mathbf{u}_+ - \mathbf{u}_-)\right] + \frac{1}{c}\partial_t \mathbf{E}, \tag{11}$$

where $D_t \equiv \partial_t + (\mathbf{U}_0, \nabla)$ is the *convective* derivative over the velocity vector field $\mathbf{U}_0$, and $C_s^{\pm} \equiv (\partial P^{\pm}/\partial(mn^{\pm}))^{1/2}$ is the sound speed for each species. We also assumed that in equilibrium $n_0^+ = n_0^- \equiv n_0$, and the two sound speeds are equal for the mean flow.

Let us now define the following set of *one-fluid* variables:

$$O\rho_0 \equiv 2mn_0, \tag{12a}$$

$$\rho \equiv m(n_+ + n_-), \tag{12b}$$

$$\rho_e \equiv e(n_+ - n_-), \tag{12c}$$

$$\mathbf{j} \equiv en_0(\mathbf{u}_+ - \mathbf{u}_-), \tag{12d}$$

$$\mathbf{v} \equiv (\mathbf{u}_+ + \mathbf{u}_-)/2. \tag{12e}$$

In these variables (note that $\rho_0 \mathbf{v} = mn_0(\mathbf{u}_+ + \mathbf{u}_-)$), the linearized *two-fluid* equations become the following set of *one-fluid* equations:

$$D_t \rho + \rho_0 \nabla \cdot \mathbf{v} = 0, \tag{13}$$

$$D_t \rho_e + \nabla \cdot \mathbf{j} = 0, \tag{14}$$

$$\rho_0[D_t \mathbf{v} + (\mathbf{v}, \nabla)\mathbf{U}_0] = -C_s^2 \nabla \rho + \frac{1}{c}\mathbf{j} \times \mathbf{B}_0, \tag{15}$$

$$D_t\mathbf{j} + (\mathbf{j},\nabla)\mathbf{U}_0 = -C_s^2\nabla\rho_e + \left(\frac{e}{m}\right)^2 \rho_0 \left[\mathbf{E} + \frac{1}{c}(\mathbf{U}_0\times\mathbf{B} + \mathbf{v}\times\mathbf{B}_0)\right], \tag{16}$$

$$\nabla\cdot\mathbf{E} = 4\pi\rho_e, \tag{17}$$

$$c\nabla\times\mathbf{E} = -\partial_t\mathbf{B}, \tag{18}$$

$$\nabla\cdot\mathbf{B} = 0, \tag{19}$$

$$c\nabla\times\mathbf{B} = 4\pi\rho_e\mathbf{U}_0 + 4\pi\mathbf{j} + \partial_t\mathbf{E}. \tag{20}$$

Hereafter the plasma will be assumed to be: (a) *cold* $C_s^2 = 0$, and (b) *nonrelativistic*. The latter assumption, $(\partial_t\mathbf{E} \simeq 0)$ simplifies Eq. (20) to

$$\mathbf{j} \approx (c/4\pi)\nabla\times\mathbf{B} - \rho_e\mathbf{U}_0, \tag{21}$$

implying $[\mathbf{U}_0\times\mathbf{B}_0 = 0]$

$$\mathbf{j}\times\mathbf{B}_0 = -(c/4\pi)\left[\nabla(\mathbf{B},\mathbf{B}_0) - (\mathbf{B}_0,\nabla)\mathbf{B}\right], \tag{22}$$

which, in turn, immediately converts the equation of motion (15) into its standard form relating the variables $\mathbf{v}$ and $\mathbf{B}$,

$$D_t\mathbf{v} + (\mathbf{v},\nabla)\mathbf{U}_0 = (v_A^2/B_0)(\partial_x\mathbf{B} - \nabla B_x), \tag{23}$$

where $v_A^2 \equiv B_0^2/4\pi\rho_0 = B_0^2/8\pi m n_0$.

Derivation of the *induction equation* for the magnetic field—another vector equation which links the magnetic field and velocity perturbations—is straightforward but tedious. A very general form [Eq. (A8)] is derived in Appendix A. For the Alfvén wave physics, it is quite adequate to assume that the plasma is quasineutral, i.e., $\rho_e = 0$. Further simplification results if $\mathbf{U}_0$ is a *linear* function of coordinates; the last term in (A8) then, is zero, and the induction equation reduces to

$$D_t\left(\mathbf{B} - \lambda^2\Delta\mathbf{B}\right) = (\mathbf{B} - \lambda^2\Delta\mathbf{B},\nabla)\mathbf{U}_0 + (\mathbf{B}_0,\nabla)\mathbf{v} - \mathbf{B}_0(\nabla\cdot\mathbf{v}) + \lambda^2(\nabla\times\mathbf{U}_0,\nabla)(\nabla\times\mathbf{B}). \tag{24}$$

Note that when the collisionless skin depth $\lambda$ is small enough, Eq. (24) further reduces to the more familiar form used in standard MHD,

$$D_t \mathbf{B} = (\mathbf{B}, \nabla)\mathbf{U}_0 + (\mathbf{B}_0, \nabla)\mathbf{v} - \mathbf{B}_0(\nabla \cdot \mathbf{v}). \tag{25}$$

In the next section, we shall use the closed set of Eqs. (13), (23), and (24) along with the no monopole condition Eq. (19).

# 3 Velocity Shear and Alfvén Waves

In this section, we solve a model problem to illustrate a variety of shear-induced physical effects. We consider a simple unidirectional mean flow $\mathbf{U}_0 \equiv (Ay,\ 0,\ 0)$, with a linear shear profile along the $Y$-axis. For this case, $D_t \equiv \partial_t + Ay\partial_x$, and $\nabla \times \mathbf{U}_0 = -A\hat{\mathbf{e}}_z$. The system of relevant equations can now be written in the explicit form,

$$(\partial_t + Ay\partial_x)\rho + \rho_0(\partial_x v_x + \partial_y v_y + \partial_z v_z) = 0, \tag{26}$$

$$\partial_x B_x + \partial_y B_y + \partial_z B_z = 0, \tag{27}$$

$$(\partial_t + Ay\partial_x)v_x + Av_y = 0, \tag{28}$$

$$(\partial_t + Ay\partial_x)v_y = (v_A^2/B_0)[\partial_x B_y - \partial_y B_x], \tag{29}$$

$$(\partial_t + Ay\partial_x)v_z = (v_A^2/B_0)[\partial_x B_z - \partial_z B_x], \tag{30}$$

$$(\partial_t + Ay\partial_x)[(1 - \lambda^2\Delta)B_y] = B_0\partial_x v_y - A\lambda^2\partial_z(\partial_z B_x - \partial_x B_z), \tag{31}$$

$$(\partial_t + Ay\partial_x)[(1 - \lambda^2\Delta)B_z] = B_0\partial_x v_z - A\lambda^2\partial_z(\partial_x B_y - \partial_y B_x). \tag{32}$$

Equations (26)–(32) define a model linear problem. Conventional 'stability' analysis of this system will revolve around an eigenmode analysis—the eigenmodes being the time asymptotic modes of oscillation that this system can sustain. In this generally valid and

powerful approach the transient behavior of the perturbations never figures, because as time goes to infinity, only normal modes propagate. It turns out, however, that for a class of linear operators,[11] the conventional normal mode analysis may not reveal the entire richness of the dynamics; in fact, extremely crucial aspects of the time evolution of the perturbations may be altogether missed. For instance, a very large transient amplification could drive a system to a nonlinear turbulent state while the normal mode analysis for the same system would predict complete stability and hence no possible transition to turbulence.

Recent investigations show that shear flows (the system under discussion) display interesting dynamical behavior which will be completely missed in a normal mode analysis [Refs. 11–15]. These aspects, generally pertaining to the details of transient dynamics, are much better elucidated by solving an initial value problem. This approach, called the nonmodal analysis, will be followed in this paper.

To "set up" the nonmodal analysis, we make the following transformation of variables,

$$x_1 = x - Ayt; \quad y_1 = y; \quad z_1 = z; \quad t_1 = t. \tag{33}$$

It is well known[11] that this transformation, a change from the Eulerian to the Lagrangian frame, leads to immense simplification in the solution of the initial-value problem.

In these new coordinates, the relevant equations take the form:

$$\partial_{t_1}\rho + \rho_0\left[\partial_{x_1}v_x + (\partial_{y_1} - At_1\partial_{x_1})v_y + \partial_{z_1}v_z\right] = 0, \tag{34}$$

$$\partial_{x_1}B_x + (\partial_{y_1} - At_1\partial_{x_1})B_y + \partial_{z_1}B_z = 0, \tag{35}$$

$$\partial_{t_1}v_x + Av_y = 0, \tag{36}$$

$$\partial_{t_1}v_y = (v_A^2/B_0)[\partial_{x_1}B_y - (\partial_{y_1} - At_1\partial_{x_1})B_x], \tag{37}$$

$$\partial_{t_1}v_z = (v_A^2/B_0)[\partial_{x_1}B_z - \partial_{z_1}B_x], \tag{38}$$

$$\partial_{t_1}[(1 - \lambda^2\Delta)B_y] = B_0\partial_{x_1}v_y - A\lambda^2\partial_{z_1}\left[\partial_{z_1}B_x - \partial_{x_1}B_z\right], \tag{39}$$

$$\partial_{t_1}[(1-\lambda^2\Delta)B_z] = B_0\partial_{x_1}v_z - A\lambda^2\partial_{z_1}\left[\partial_x B_y - (\partial_{y_1} - At_1\partial_{x_1})B_x\right], \tag{40}$$

where $\Delta = \partial^2_{x_1} + (\partial_{y_1} - At_1\partial_{x_1})^2 + \partial^2_{z_1}$.

We may further expand the perturbations as

$$F = \int dk_{x_1}dk_{y_1}dk_{z_1}\widehat{F}(k_{x_1},k_{y_1},k_{z_1},t_1)\exp[i(k_{x_1}x_1 + k_{y_1}y_1 + k_{z_1}z_1)], \tag{41}$$

and introduce the following dimensionless quantities: $R \equiv A/v_A k_{x_1}$, $\tau \equiv v_A k_{x_1} t_1$, $\beta_0 \equiv k_{y_1}/k_{x_1}$, $\beta(\tau) \equiv \beta_0 - R\tau$, $\gamma \equiv k_{z_1}/k_{x_1}$, $v_{x,y,z} \equiv \widehat{v}_{x,y,z}/v_A$, $b_{x,y,z} \equiv i\widehat{B}_{x,y,z}/B_0$, $\epsilon^2 \equiv \lambda^2 k^2_{x_1}$, and $M^2(\tau) \equiv 1 + \beta^2(\tau) + \gamma^2$.

In the new notation, (35) gives an algebraic relation between the dimensionless components of the magnetic field perturbation,

$$b_x = -\beta b_y - \gamma b_z. \tag{42}$$

This relation, in turn, allows us to convert (37)–(40) into a closed set of first order ordinary differential equations (ODEs) for the "transverse" (with respect to $\mathbf{B}_0$) variables $v_y$, $v_z$, $b_y$, and $b_z$:

$$\partial_\tau v_y = [1+\beta^2]b_y + \gamma\beta b_z, \tag{43}$$

$$\partial_\tau v_z = [1+\gamma^2]b_z + \gamma\beta b_y, \tag{44}$$

$$\partial_\tau[(1+\epsilon^2M^2)b_y] = -v_y - R\epsilon^2\gamma[(1+\gamma^2)b_z + \gamma\beta b_y], \tag{45}$$

$$\partial_\tau[(1+\epsilon^2M^2)b_z] = -v_z + R\epsilon^2\gamma[(1+\beta^2)b_y + \gamma\beta b_z]. \tag{46}$$

These equations may be rearranged in the following way,

$$\partial_\tau\left[(1+\epsilon^2M^2)b_y + R\epsilon^2\gamma v_z\right] = -v_y, \tag{47}$$

$$\partial_\tau\left[(1+\epsilon^2M^2)b_z - R\epsilon^2\gamma v_y\right] = -v_z. \tag{48}$$

Notice that the remaining variables $v_x$ and $D \equiv i\widehat{\rho}/\rho_0$, can be determined through [see Eqs. (34) and (36)]

$$\partial_\tau D = v_x + \beta v_y + \gamma v_z, \tag{49}$$

$$\partial_\tau v_x = -R v_y, \tag{50}$$

once the 'transverse' variables are known. In addition, Eqs. (47) and (50) connect $v_x$ with $b_y$ and $v_z$ by the following algebraic relation:

$$R(1+\epsilon^2 M^2) b_y - v_x + R^2 \epsilon^2 \gamma v_z = \text{const.} \tag{51}$$

We now introduce an appropriate 'measure' of the spectral energy density of spatial Fourier harmonics,

$$\mathcal{E}(\tau) \equiv \frac{|v_x|^2 + |v_y|^2 + |v_z|^2}{2(1+\epsilon^2 M^2)} + \frac{|b_x|^2 + |b_y|^2 + |b_z|^2}{2}, \tag{52}$$

which includes the kinetic energy of the plasma, the energy of the magnetic field, and also the energy of the electric field. The latter evokes the factor $(1+\epsilon^2 M^2)$ in the denominator of the first term. Clearly, when $\epsilon \ll 1$, the energy of the electric field is $(v/c)^2$ times less than the fluctuating magnetic field energy (as in usual MHD) and (52) reduces to a sum of only the kinetic and magnetic energies. The spectral energy density $\mathcal{E}(\tau)$ is defined in such a way that for the "no shear" $(R = 0)$ limit, it is a conserved quantity:

In terms of the auxiliary quantities

$$A_y \equiv (1+\epsilon^2 M^2) b_y, \tag{53a}$$

$$A_z \equiv (1+\epsilon^2 M^2) b_z, \tag{53b}$$

Eqs. (43)–(46) may be written as an equivalent system,

$$\partial_\tau v_y = \frac{1}{1+\epsilon^2 M^2} \left[ (1+\beta^2) A_y + \gamma\beta A_z \right], \tag{54}$$

$$\partial_\tau v_z = \frac{1}{1+\epsilon^2 M^2}\left[(1+\gamma^2)A_z + \gamma\beta A_y\right], \tag{55}$$

$$\partial_\tau A_y = -v_y - \frac{R\epsilon^2\gamma}{1+\epsilon^2 M^2}\left[(1+\gamma^2)A_z + \gamma\beta A_y\right], \tag{56}$$

$$\partial_\tau A_z = -v_z + \frac{R\epsilon^2\gamma}{1+\epsilon^2 M^2}\left[(1+\beta^2)A_y + \gamma\beta A_z\right]. \tag{57}$$

Before proceeding to the next section where we solve various special cases of this general problem [Eqs. (43)–(46), or (54)–(57)], it is interesting to realize that one can readily eliminate $v_y$ and $v_z$ in Eqs. (43)–(46) to obtain the following coupled pair of second order ODE's for the transverse components of magnetic field perturbations ($b_y$ and $b_z$):

$$\partial_\tau^2 b_y + \left[\frac{\epsilon^2 R\beta(\gamma^2-4)}{1+\epsilon^2 M^2}\right]\partial_\tau b_y + \left[\frac{(1+\beta^2)+\epsilon^2R^2(2-\gamma^2)}{1+\epsilon^2M^2}\right] b_y$$
$$= -\left[\frac{\gamma\beta}{1+\epsilon^2M^2}\right] b_z - \left[\frac{R\epsilon^2\gamma(1+\gamma^2)}{1+\epsilon^2M^2}\right]\partial_\tau b_z, \tag{58}$$

$$\partial_\tau^2 b_z - \left[\frac{\epsilon^2 R\beta(\gamma^2+4)}{1+\epsilon^2 M^2}\right]\partial_\tau b_z + \left[\frac{(1+\gamma^2)+\epsilon^2R^2(2+\gamma^2)}{1+\epsilon^2M^2}\right] b_z$$
$$= -\left[\gamma\beta(1+2R^2\frac{\epsilon^2)}{1+\epsilon^2M^2}\right] b_y + \left[\frac{R\epsilon^2\gamma(1+\beta^2)}{1+\epsilon^2M^2}\right]\partial_\tau b_y. \tag{59}$$

## 3.1 "Zero Shear" $(R = 0)$ case

In spite of the relative simplicity of the system (two-coupled second order ODE's), analytical progress requires further simplifying assumptions. We begin by studying the well-known shearless flow, $R = 0$.

In this case the system of equations simplify enormously. From (58) and (59) one gets:

$$\partial_\tau^2 b_y + \omega_1^2 b_y + \alpha b_z = 0, \tag{60}$$

$$\partial_\tau^2 b_z + \omega_2^2 b_z + \alpha b_y = 0, \tag{61}$$

where $\omega_1^2 \equiv (1+\beta_0^2)/(1+\epsilon^2 M_0^2)$, $\omega_2^2 \equiv (1+\gamma^2)/(1+\epsilon^2 M_0^2)$, and $\alpha \equiv \gamma\beta_0/(1+\epsilon^2 M_0^2)$.

The normal frequencies of these oscillations, calculated by the standard formula

$$\Omega_{\pm}^2 \equiv \frac{1}{2}\left[(\omega_1^2+\omega_2^2) \pm \sqrt{(\omega_1^2-\omega_2^2)^2+4\alpha^2}\right], \tag{62}$$

are equal to

$$\Omega_c^2 \equiv \Omega_+^2 = \frac{1+\gamma^2+\beta_0^2}{1+\epsilon^2 M_0^2}, \tag{63}$$

$$\Omega_s^2 \equiv \Omega_-^2 = \frac{1}{1+\epsilon^2 M_0^2}, \tag{64}$$

and may easily be identified respectively with *compressional*, and *shear Alfvén wave* frequencies.[16,17] In dimensional notation, the frequencies take the familiar form,

$$\overline{\Omega}_c^2 \equiv k_{x_1}^2 v_A^2 \Omega_c^2 = \frac{v_A^2 k^2}{1+\lambda^2 k^2}, \tag{65}$$

$$\overline{\Omega}_s^2 \equiv k_{x_1}^2 v_A^2 \Omega_s^2 = \frac{v_A^2 k_{x_1}^2}{1+\lambda^2 k^2}. \tag{66}$$

It is easy to show that $b_x$ and $\psi \equiv \gamma b_y - \beta_0 b_z$ obey

$$\partial_\tau^2 b_x + \Omega_c^2 b_x = 0, \tag{67}$$

$$\partial_\tau^2 \psi + \Omega_s^2 \psi = 0, \tag{68}$$

which are linearly independent. As expected, the shearless system is characterized by two fundamental normal modes with well-known eigenfrequencies $\Omega_c$ and $\Omega_s$.

## 3.2 Two-dimensional Waves ($\gamma = 0$)

The shearless case is standard and relatively uninteresting. Let us now turn the shear on ($R \neq 0$), but consider another simple case for which the perturbations are two-dimensional (2-D), i.e., $k_{z_1} = 0$ ($\gamma = 0$). In this case $M^2(\tau) = 1+\beta^2(\tau)$, and (54)–(57) can be manipulated to give

$$\partial_\tau^2 A_y + \left[\frac{1+\beta^2}{1+\epsilon^2(1+\beta^2)}\right] A_y = 0, \tag{69}$$

and

$$\partial_\tau^2 A_z + \left[\frac{1}{1+\epsilon^2(1+\beta^2)}\right] A_z = 0. \tag{70}$$

These equations describe 'oscillations' with variable frequencies $\omega_c^2(\tau) \equiv (1+\beta^2)/[1+\epsilon^2(1+\beta^2)]$ and $\omega_s^2(\tau) \equiv 1/[1+\epsilon^2(1+\beta^2)]$. These can be (for 2-D perturbations) again viewed as the compressional and shear Alfvén frequencies respectively. For sufficiently small values of $R$, these frequencies vary slowly (adiabatically) and the approximate analytic solutions of (69) and (70) may be written as[12]:

$$A_y(\tau) = \frac{C_1}{\sqrt{\omega_c(\tau)}} \exp[i(\phi_c(\tau) + \phi_{c0})], \tag{71a}$$

$$A_z(\tau) = \frac{C_2}{\sqrt{\omega_s(\tau)}} \exp[i(\phi_s(\tau) + \phi_{s0})], \tag{71b}$$

where the amplitudes of these modes are determined through the corresponding adiabatic invariants: $C_1 \equiv a_c^2(\tau)\omega_c(\tau)$ and $C_2 \equiv a_s^2(\tau)\omega_s(\tau)$; $C_1$ and $C_2$, though products of two time varying quantitiies, are constants with their values determined by the initial conditions. The phases are given by

$$\phi_{c,s}(\tau) \equiv \int \omega_{c,s}(\tau) d\tau. \tag{72}$$

It is easy to find that the amplitudes of all physical variables may be expressed through the amplitudes of $A_y$ and $A_z$. In particular, $|v_x| = R|A_y|$, $|v_y| \simeq \omega_c|A_y|$, $|v_z| \simeq \omega_s|A_z|$, $|b_x| = |\beta|\omega_s^2|A_y|$, $|b_y| = \omega_s^2|A_y|$, and $|b_z| = \omega_s^2|A_z|$. Using these expressions, together with (52), (71a), and (71b), we can derive the following important *analytic* expression for the spectral energy density:

$$\mathcal{E}(\tau) \simeq \omega_s^2(\tau)\left[C_1^2\omega_c(\tau) + C_2^2\omega_s(\tau)\right]. \tag{73}$$

This is an approximate equation, but it is found to work excellently when $R \ll 1$. In Figs. 1 and 2 we present results of a direct numerical integration of the general, unsimplified defining equations for the following set of parameters: $\beta_0 = 10$, $R = 0.1$, and $\epsilon = 0.5$. The

initial perturbation, corresponding to Fig. 1, consists of a pure compressional Alfvén mode. The frequency of the perturbation is given by $\omega_c(\tau)$, while the corresponding amplitude (envelope function) is $a_c(\tau) \equiv C_1/\sqrt{\omega}_c(\tau)$. Figure 1(a) shows that in time periods of interest, the amplitude of $b_y(\tau)$ increases by well over an order of magnitude. Corresponding graph for $\mathcal{E}(\tau)$ is presented in Figure 1(b). The solid line displays the results of the numerically calculated $\mathcal{E}(\tau)$, while the circles represent $\mathcal{E}(\tau)$ calculated by the approximate equation (73). The excellent agreement between the exact and approximate solutions is evident, and it pertains even when the initial conditions are changed from a pure compressional to a pure shear Alfvén mode [see Figs. 2(a) and (b)] or to some admixture of these two modes.

The dip at $\tau = 100$ in Eq. 1b is just a consequence of the detailed time dependence of $\omega_s^2(\tau)\omega_c(\tau)$ [which determines $\mathcal{E}(\tau)$ for $C_2 = 0$, and has no other physical significance. Another manifestation of the time dependence of $\omega_s^2(\tau) = [1 + \epsilon^2[1 + (B_0 - R\tau)^2]^{-1}$ which, for $\beta_0, R_0 > 0$, has a maximum at $\tau = \tau_* \equiv \beta_0/R$, is displayed in Fig. 2a; the oscillations are most rapid at $\tau = \tau_*$ ($\sim 100$ for the examaple shown) and slow down on either side of $\tau_*$.

Results of the numerical calculations, as well as those of direct evaluations by the approximate formula (73) show that 2-D perturbations for sufficiently large values of $\epsilon$ ($\epsilon \geq 0.1$), exhibit quite strong (up to several orders of magnitude) *transient amplifications*. In fact, the ratio of the spectral energy at $\tau = \tau_*$ [$\tau_*$ corresponds to the moment, when the time dependent component of the wave number vector $k_y(\tau) = k_{y_1} - At_1 k_{x_1}$ changes its sign. Because of the asymmetry introduced by shear, the direction of k becomes significant] to the initial energy (at $\tau = 0$) may be readily found from (73) to be

$$\frac{\mathcal{E}(\tau_*)}{\mathcal{E}(0)} = \left[\frac{1 + \epsilon^2(1 + \beta_0^2)}{1 + \epsilon^2}\right]^{3/2} \frac{C_1^2 + C_2^2}{C_1^2\sqrt{1 + \beta_0^2} + C_2^2}. \tag{74}$$

This expression clearly shows that the substantial transient growth of the perturbation energy is a strong function of the initial orientation of the $\mathbf{k}$ vector (value of $\beta_0$), and of the value of the dimensionless skin depth parameter $\epsilon$. For large enough values of $\epsilon_0\beta_0$,

Eq. (74) predicts large amplification factors. For $C_1 = 0$, $\epsilon = .25, \beta_0 = 10$, for example, $\mathcal{E}(T_*)/\mathcal{E}(0) \sim 26\sqrt{26} \sim 100$. On the other hand, the amplification factor does not depend directly on the strength of the ambient magnetic field $\mathbf{B}_0$.

Note that for large enough values of $\tau$ ($\tau \gg \tau_*$) the shear Alfvén wave frequency $\omega_s$ tends to zero, while $\omega_c$ asymptotically approaches the cyclotron frequency for the $e^+e-$ plasma. In other words, the shear-induced "linear drift" of the perturbations[11-15] leads to the asymptotic transition of the compressional Alfvén waves into the cyclotron waves. Going back to the specified evolution equations for the physical variables, we can easily show that in this asymptotic regime, amplitudes of all components of the magnetic field perturbations and $v_z$ tend to zero, while the amplitudes of $v_x$ and $v_y$ attain constant values.

For the shear Alfvén mode the phase integral (72) can be evaluated in terms of elementary functions leading to the explicit solution

$$A_z(\tau) = A_z(0) \left( \frac{1 + \epsilon^2(1+\beta^2)}{1 + \epsilon^2(1+\beta_0^2)} \right)^{1/4} \cos\left( \frac{1}{\epsilon R} \ln\left( \frac{\epsilon\beta_0 + \sqrt{1 + \epsilon^2(1+\beta_0^2)}}{\epsilon\beta + \sqrt{1 + \epsilon^2(1+\beta^2)}} \right) \right). \tag{75}$$

The analytical results are, of course, meaningful only when the frequencies vary slowly (adiabatically) with time. Applicability of the adiabatic approximation is governed by the conditions:

$$|\partial_\tau \omega_{c,s}(\tau)| \ll \omega_{c,s}^2(\tau), \tag{76a}$$

which hold for small enough values of the $R$ parameter. For the case of the shear Alfvén mode, condition

$$\epsilon^2 R|\beta| \ll \left[1 + \epsilon^2(1+\beta^2)\right]^{1/2}, \tag{76b}$$

while for the compressional Alfvén mode it reads:

$$R|\beta| \ll (1+\beta^2)^{3/2} \left[1 + \epsilon^2(1+\beta^2)\right]^{1/2}. \tag{76c}$$

As an aside, it is worth mentioning that in terms of the new independent variable

$$T \equiv -\epsilon^2(\beta_0 - R\tau)^2/(1+\epsilon^2), \tag{77}$$

we can reduce (70) to the *Gauss Hypergeometric* equation[18]:

$$4z(1-z)\partial_T^2 A_z + 2(1-z)\partial_T A_z - CA_z = 0, \tag{78}$$

where $C \equiv 1/\epsilon^2 R^2$.

## 3.3 Three-Dimensional Waves with $\lambda \ll 1$

For high density plasmas, there exists a broad range of wavenumbers for which $|\lambda^2 \Delta| \ll 1$, and can be neglected. In this case, (58)–(59) reduces to the following pair of equations:

$$\partial_\tau^2 b_y + (1+\beta^2) b_y + \gamma\beta b_z = 0, \tag{79}$$

$$\partial_\tau^2 b_z + (1+\gamma^2) b_z + \gamma\beta b_y = 0, \tag{80}$$

which are similar to (60)–(61). The essential difference here is that now we have $\beta(\tau)$'s instead of $\beta_0$'s and, hence, the coupling coefficient and one of the eigenfrequencies are *time dependent*: $\omega_1^2(\tau) \equiv 1+\beta^2$, $\omega_2^2 \equiv 1+\gamma^2$, $\alpha(\tau) \equiv \gamma\beta$. The 'normal frequencies' of these oscillations, calculated again by (62), are:

$$\Omega_c^2(\tau) \equiv \Omega_+^2 = 1 + \gamma^2 + \beta^2, \tag{81}$$

$$\Omega_s^2 \equiv \Omega_-^2 = 1, \tag{82}$$

and may easily be termed as *compressional,* and *shear Alfvén wave* frequencies respectively. However, this time, the frequency of the compressional Alfvén wave is *time dependent* and only when $R \ll 1$, it would vary adiabatically.

The system under investigation is mathematically equivalent to a pair of linear pendulums, connected by a spring with a varying stiffness coefficient $[\alpha(\tau) = \gamma\beta(\tau)]$. The length of one of these pendula also varies in time. Strictly speaking, due to this variation, the canonical theory of coupled oscillations is no longer valid. However, when $\omega_1(\tau)$ and $\alpha(\tau)$

vary slowly (adiabatically), as they do when $R \ll 1$, the standard theory of coupled oscillations may serve as a useful guide in understanding and interpreting the inherent physical processes.

A rather similar mechanical problem was investigated in.[19] It was pointed out that for an effective energy exchange to occur between two weakly coupled pendulums, the following conditions must be satisfied:

- (A) There should exist a so called "degeneracy region," (DR) where

$$|\Omega_+^2 - \Omega_-^2| \leq |\alpha(\tau)|, \tag{83}$$

- (B) the DR should be "passed" slowly—the traversal time should be much greater than the period of the beats:

$$|\partial_\tau \Omega_+(\tau)| \ll |\alpha(\tau)|. \tag{84}$$

It is easy to notice that in our case the difference $\Omega_+(\tau) - \Omega_-(\tau)$ attains its minimum value at $\tau = \tau_*(= \beta_0/R)$. It is, therefore, evident that the DR is in the neighborhood of $\tau_*$ (at times, when $0 < |\beta(\tau)| < 1$). In the vicinity of $\tau = \tau_*$, $\gamma < 1$ leads to the most efficient mode coupling, and hence to the possibility of mutual transformation of the modes. It can be readily seen that condition (84) holds in DR when $R \ll 1$.

The "adiabatic behavior" of the modes implies that they should normally follow the dispersion curves of their own: spectral energy density (52) of either the shear Alfvén mode ($\mathcal{E}_-(\tau)$) or the compressional Alfvén mode ($\mathcal{E}_+(\tau)$) should be proportional to its corresponding frequency $\mathcal{E}_\pm \sim \Omega_\pm$[19,13,15]. This mode of energy evolution, however, will not pertain in DR, where efficient transformation of one wave into the other occurs. For instance, as we see from Figs. 3 and 4, the energy of an initially excited shear Alfvén mode increases approximately by the $\mathcal{E}_-(\tau) \sim \Omega_-(\tau)$ law up to the vicinity of the point $\tau_*$, where it is partially transformed into compressional Alfvén mode. Afterwards, its energy evolution would still proceed adiabatically, but now according to the law: $\mathcal{E}_+(\tau) \sim \Omega_+(\tau)$.

The salient features of the richness of the structures shown in Figs. 3–4 [$\beta_0 = 10, R = 0.1, \epsilon = 5 \times 10^{-3}$, and $\gamma = 0.1 (\gamma = 1)$] can be readily understood by examining the approximate analytical expressions for the frequencies and the amplitudes. In both these cases, an initial shear wave [$\Omega_s^2 = 1$], at times $\tau \sim \tau_* \ (= 100)$, begins transforming into a compressional wave whose frequency $\Omega_c = [1 + r^2 + (\beta - R_0 \tau)^2]^{1/2} = [1 + r^2 + R_0^2 (\tau_* - \tau)^2]^{1/2}$ tends to increase as $\tau > \tau_*$, and can become much greater than $|\Omega_s|$ for large enough times. The compressional wave, generated by the shear induced coupling, becomes the dominant mode after $\tau > 120$ for Fig. 3a.

The only difference between the two cases is the magnitude of $\gamma$ which determines the efficiency of coupling. It is clear that the transformation of the shear into the compressional mode is visibly more pronounced and happens earlier for $\gamma = 0.1$ as compared to $\gamma = 1$. That is precisely the reason why Fig. 3a is so asymmetric in time—the initial shear wave for $\tau < \tau_*$ is almost fully converted into a compressional wave for $\tau > \tau_*$. The plot in Fig. 4a, on the other hand, retains the symmetry of Fig. 2a, because, due to poor conversion-efficiency, the initial shear wave gets contaminated by only a small admixture of compressional wave even for times in excess of $\tau_*$.

It is again the difference in conversion efficiency, which accounts for the obvious differences in the energy plots given in Figs. 3b and 4b respectively. For 3b, at times $\tau \gtrsim \tau_*$, the conversion to the compressional wave is almost complete. Afterwards the energy increases rapidly because $E(\tau)$ for this mode scales with $\Omega_c(\tau)$ which increases almost linearly with time for $\tau > \tau_*$. The behavior of the $E(\tau)$ shown in Fig. 4b is a little more complicated. The sudden increase in energy at $\tau = \tau_*$ is the usual increase for the energy of the shear wave as a function of time [see Fig. 2b, for comparison]. The gradual overall rise after $\tau = \tau_*$, however, is due to the energy contributed by the newly generated small amplitude compressional wave. The involved structure of $E(\tau)$ near $\tau = \tau_*$ is due to the fact that in this region [DR, the region of mode conversion], the energy associated with a mode is not merely proportional to

the mode frequency.

It should be noted that for the case, considered in this subsection, $b_x$ and $\psi \equiv \gamma b_y - \beta b_z$ obey coupled equations

$$\partial_\tau^2 b_x + \Omega_c^2 b_x = -2Rv_y, \tag{85}$$

$$\partial_\tau^2 \psi + \Omega_s^2 \psi = -2Rv_z, \tag{86}$$

which reduce to (67)–(68) for $R = 0$. Equations (85)–(86) clearly show that in the nonzero shear case, the compressional and the shear Alfvén modes *are* intrinsically coupled; the strength of coupling is measured by $R$.

It is, therefore, evident that under certain circumstances (existence of the "degeneracy region," and the satisfaction of the "slow pass" conditions) the modes may effectively transform into each other with a corresponding energy transfer. The strong interaction of the modes is insured by sufficiently large values of $\beta_0$ (of $k_y$) and $\epsilon$. The transient amplication is further enhanced by a smaller $\gamma$ (smaller $k_z$). For a given $k_x$, larger $k_y$ and smaller $k_z$ lead to the most spectacular results. The compressional mode is able to extract energy from the mean shear flow continuously (at $\tau > \tau_*$) and in this feature it closely resembles the plain sound wave whose evolution has been studied earlier.[12]

# 4 Discussion and Speculations of Astrophysical Interest

The results presented in the previous section show that even in the simplest $e^+e^-$ plasma shear flow—the parallel flow of a cold and nonrelativistic plasma—the presence of the shear leads to new physical processes notably changing the evolution of oscillation modes in the plasma, and causing their interaction with each other and with the mean (bulk) flow. Main results of our investigation are:

- Two-dimensional (2-D) perturbations ($\gamma = 0$), localized in the $X$-$Y$ plane, exhibit adiabatic evolution (for $R \ll 1$) when their amplitude and frequency (phase) characteristics vary slowly (adiabatically) in time. Under certain conditions (determined, for example, by the initial orientation of the $\mathbf{k}$ vector and by the value of skin depth parameter $\epsilon$), large transient growths, up to several order of magnitude, are possible.

- Three-dimensional (3-D) perturbations, (with $\gamma \neq 0$) are physically coupled with one another via the shear parameter $R$. The coupling remains strong even for perturbations with a wavelength much longer than the collisionless skin depth. This coupling leads to a mutual transformation of the shear Alfvén and the compressional Alfvén waves in a cold nonrelativistic plasma. Transient amplification of the modes is also found. The efficiency of mutual transformation is greater for small $\gamma$.

- For the general case, when no constraints are put onto the flow and perturbation parameters, one may expect the complex interplay of the effects mentioned in the previous two paragraphs.

These features of the wave dynamics in the $e^+e^-$ plasma may prove to be quite significant in advancing our understanding of the processes taking place in the pulsar magnetosphere and the pulsar wind.

To appreciate this connection, we make a short digression. It is generally agreed that the processes of radio emission from the pulsars are still poorly understood (see, for the most recent review,[2] and references therein); there does not exist a widely accepted theoretical model. Although an $e^+e^-$ plasma is thought to be a possible candidate for the radio emission, not too much is known either about the location of the assumed sources of the $e^+e^-$ plasma ("gaps") or about the details of the plasma production processes. Furthermore, it is impossible to predict the velocity distribution of particles; a knowledge which is critical for the identification of a 'workable' emission mechanism.

However, there are some general aspects of the phenomenon, which can be specified with some certainty. In particular, it *is* known that the $e^+e^-$ plasma is produced in the polar cap regions at some height above the surface of the neutron star and, that the secondary plasma involves electrons and positrons flowing outward along the open field lines. It is also known that the pulsar radio emission is characterized by prominently high brightness temperatures ($T_b \sim 10^{25} - 10^{30}$ K), thus requiring some sort of a *coherent* emission mechanism.

The broad literature on pulsar radio emission problem contains several proposed models based, generally, on three kinds of plasma processes[20,2]: antenna mechanisms, reactive instabilities and maser mechanisms. Currently the most preferred emission mechanism for pulsars is the maser mechanism, or the relativistic plasma emission. The mechanism operates in two stages: 1) an instability that generates Langmuir-like or Alfvén-type waves that cannot escape to infinity and, 2) some kind of *nonlinear* "conversion process" that transforms a part of the energy of these waves into the escaping radiation.[21,2]

There are several empirical observations which any proposed mechanism must respect[2]:

- The mechanism should not be strongly dependent on the strength of the pulsar magnetic field $B$: it should apply with equal success to both weak-B (millisecond) and strong-B (young, fast) pulsars;

- Coherent emission should occur in many localized, *transient* subsources. It implies that the optimum model should describe the origin and characteristics of these subsources;

- The mechanism should contain a guaranteed "feedback." In the case of the relativistic plasma emission, for instance, a continuous "pump" (overtaking of slower particles by faster particles) is needed for the maintenance of those features of the particle distribution function, which are responsible for the maser process.

It would, thus, appear that in this connection the shear induced processes which ensure natural, safe and effective transfer of the mean $e^+e^-$ plasma flow energy into the energy of

the excited linear waves, may be worth exploring. We have demonstrated that the evolution of these waves is strongly influenced by the shear forces: coupling of various wave modes, their resulting mutual transformation and corresponding energy exchange allows the flow energy to be eventually converted into a mode of choice which can escape as radiation.

A most notable characteristic of these processes, in the context of their possible relevance to pulsar plasma physics, is that they are quite insensitive to the strength of the ambient magnetic field $\mathbf{B}_0$: efficiency of the processes described in this study mostly depend on the features of the flow, and of the nature of perturbations.

A caveat is in order here. In the present paper, we have studied the highly idealized model of a cold, nonrelativistic parallel shear flow of an $e^+e^-$ plasma. Our main focus was on the delineation of the physics relating to the effects of velocity shear on the wave dynamics. The results of this study, therefore, have only a limited direct applicability; they could, for example, be applied to the investigation of the physics of the *nonrelativistic* $e^+e^-$ laboratory plasma flows.[8] We have also generalized the basic theory to cold relativistic flows. It turns out the basic results derived in this paper survive wholly intact for cold relativistic flows that are weakly-sheared. Since the relativistic calculation is quite straightforward, it is presented in Appendix B.

We are fully aware that a quantitative determination of the velocity shear induced effects to the theory of pulsar radio emission requires the extension of this simple model to include other important physical effects, such as real geometry and kinematics of the $e^+e^-$ shear flows, plasma temperature, other plasma inhomogeneities etc. Postponing the detailed analysis of these effects to future work, we would like to stress that the velocity shear induced phenomena are interesting, and may be quite relevant to the problem of pulsar radio emission. It is conceivable that the pulsar radiation, as well as the radiation of $e^+e^-$ jets in AGN's, is energetically fuelled by the huge amount of rotational energy in the "central engines" liberated partially in the plasma outflows. We argue that, afterwards, this energy

is transferred to the excited wave-like perturbations via the "shear channel."

# Appendix A: Derivation of the Induction Equation

In order to derive the *induction equation* for the magnetic field perturbation $\mathbf{B}$ we, first of all, determine the electric field vector $\mathbf{E}$ through the generalized Ohm's law [Eq. (16)]:

$$\mathbf{E} = -(\mathbf{U}_0/c) \times \mathbf{B} - (\mathbf{v}/c) \times \mathbf{B}_0 + (m^2/e^2\rho_0)[D_t\mathbf{j} + (\mathbf{j}, \nabla)\mathbf{U}_0]. \tag{A1}$$

Next, we calculate $\nabla \times \mathbf{E}$, and insert it into Faraday's law to get the induction equation. Using Eqs. (21) and (A1), we find

$$D_t\mathbf{j} + (\mathbf{j}, \nabla)\mathbf{U}_0 = (c/4\pi)\left[D_t(\nabla \times \mathbf{B}) + (\nabla \times \mathbf{B}, \nabla)\mathbf{U}_0\right] - \mathbf{U}_0 D_t\rho_e. \tag{A2}$$

It is easy to derive the following vector identities [$\nabla \cdot \mathbf{B} = 0, \mathbf{B}_0$ is uniform]

$$\nabla \times (\mathbf{U}_0 \times \mathbf{B}) = (\mathbf{B}, \nabla)\mathbf{U}_0 - (\mathbf{U}_0, \nabla)\mathbf{B}, \tag{A3}$$

$$\nabla \times (\mathbf{v} \times \mathbf{B}_0) = (\mathbf{B}_0, \nabla)\mathbf{v} - \mathbf{B}_0(\nabla \cdot \mathbf{v}), \tag{A4}$$

$$\nabla \times [(\mathbf{U}_0, \nabla)(\nabla \times \mathbf{B}) + (\nabla \times \mathbf{B}, \nabla)\mathbf{U}_0] = -$$

$$-\nabla \times \left[\mathbf{U}_0 \times (\nabla \times (\nabla \times \mathbf{B})) + (\nabla \times \mathbf{B}) \times (\nabla \times \mathbf{U}_0)\right], \tag{A5}$$

$$\nabla \times [\mathbf{U}_0 \times (\nabla \times (\nabla \times \mathbf{B}))] = (\Delta\mathbf{B}, \nabla)\mathbf{U}_0 - (\mathbf{U}_0, \nabla)\Delta\mathbf{B}, \tag{A6}$$

$$\nabla \times [(\nabla \times \mathbf{B}) \times (\nabla \times \mathbf{U}_0)] = (\nabla \times \mathbf{U}_0, \nabla)(\nabla \times \mathbf{B}) - (\nabla \times \mathbf{B}, \nabla)(\nabla \times \mathbf{U}_0). \tag{A7}$$

All these expressions may be combined and after obvious rearranging of terms we finally get the following explicit form of the *induction equation*:

$$D_t\left[\mathbf{B} - \lambda^2\Delta\mathbf{B} - (m^2/e^2\rho_0)\nabla \times (\rho_e\mathbf{U}_0)\right] = (\mathbf{B} - \lambda^2\Delta\mathbf{B}, \nabla)\mathbf{U}_0 - \mathbf{B}_0(\nabla \cdot \mathbf{v}) + (\mathbf{B}_0, \nabla)\mathbf{v} +$$

$$+ \lambda^2\left[(\nabla \times \mathbf{U}_0, \nabla)(\nabla \times \mathbf{B}) - (\nabla \times \mathbf{B}, \nabla)(\nabla \times \mathbf{U}_0)\right], \tag{A8}$$

where $\lambda \equiv (mc^2/4\pi e^2 n_0)^{1/2}$ is the collisionless skin depth, and $\Delta \equiv \partial_x^2 + \partial_y^2 + \partial_z^2$ is the usual spatial Laplace operator.

# Appendix B: Weakly Sheared Relativistic Flow

In this appendix, we show that the problem of a weakly-sheared cold relativistic flow is mathematically entirely equivalent to the problem studied in the main text of this paper. For the sake of simplicity, we shall deal with the case when the wavelength of the modes is much larger than the collisionless skin depth, i.e., $\lambda|k| \ll 1$.

Let us assume that the ordered ambient flow is relativistic, and is characterized by $\mathbf{B}_0 = \widehat{\mathbf{e}}_x B_0$ and the momentum

$$\mathbf{P}_0 = \widehat{e}_x P_0(y). \tag{B1}$$

Naturally, this $\mathbf{P}_0$ has an associated flow velocity

$$\mathbf{U}_0 = \widehat{\mathbf{e}}_x U_0(y) = \widehat{\mathbf{e}}_x \frac{P_0(y)}{m\gamma_0(y)}, \tag{B2}$$

where $\gamma_0 = (1 + P_0^2/m^2c^2)^{1/2}$ is the standard relativistic factor. In this section, it is more convenient to write the equations of motion in terms of the canonical momenta $\mathbf{p}^{\pm}$. These are

$$\mathcal{L}\mathbf{p}^{\pm} \equiv (\partial_t + U_0(y)\partial_x)\,\mathbf{p}^{\pm} = \pm e\left[\mathbf{E} + \frac{\mathbf{U}_0 \times \mathbf{B}}{c} + \frac{\mathbf{u}^{\pm} \times \mathbf{B}_0}{c}\right], \tag{B3}$$

which are readily converted into one-fluid equations in the variables $\widehat{\mathbf{P}} = (\mathbf{p}^+ + \mathbf{p}^-)/2$, $\mathbf{U} = (\mathbf{u}^+ + \mathbf{u}^-)/2$, the current $\mathbf{J}$, the density $\rho_0 = 2mn_0$ etc. The one fluid equations from (B3) take the form

$$\mathcal{L}\widehat{P}_y = \frac{mB_0}{4\pi\rho_0}\left[\partial_x B_y - \partial_y B_x\right], \tag{B4}$$

$$\mathcal{L}\widehat{P}_z = \frac{mB_0}{4\pi\rho_0}\left[\partial_x B_z - \partial_z B_x\right], \tag{B5}$$

which, apart from a slightly complicated form of $\mathcal{L}$, are similar to (29)–(30). It is quite straightforward to evaluate the current in terms of $\mathbf{P}$'s, and then we can obtain the other two relevant equations

$$\mathcal{L}B_y = \frac{B_0}{m\gamma_0}\partial_x \widehat{P}_y, \tag{B6}$$

$$\mathcal{L}B_z = \frac{B_0}{m\gamma_0}\partial_x \widehat{P}_z, \tag{B7}$$

exactly similar in form to the $\lambda = 0$ version of (31) and (32); only $\gamma_0$ has made its appearance. Equations (B4)–(B7), along with $\nabla \cdot \mathbf{B} = 0$ form a closed linear system.

The prescription of nonmodal analysis is to make the following transformation of variables:

$$x_1 = x - U_0(y)t, \qquad y_1 = y,\ z_1 = z,\ t_1 = t \tag{B8}$$

with the derivatives $\partial_{x_1} = \partial_x$, $\partial_{z_1} = \partial_z$,

$$\mathcal{L} = \partial_t + U_0(y)\partial_x = \partial_{t_1}, \tag{B9}$$

and

$$\partial_y = \partial_{y_1} - t_1[\partial_y U_0(y)]\partial_{x_1}. \tag{B10}$$

Since the flow is supposed to be weakly sheared, we could assume

$$U_0(y) = a + Ay \tag{B11}$$

$Ad \ll a$, where $d$ is the characterstic width of the flow i.e., the flow has a strong steady directed component plus a weak varying part. Using (B10), one finds

$$\partial_y = \partial_{y_1} - At_1\partial_{x_1}, \tag{B12}$$

and one also approximates

$$\gamma_0 = (1 + P_0^2/m^2c^2)^{1/2} = (1 - U_0^2/c^2)^{-1/2} \simeq (1 - a^2/c^2)^{-1/2}. \tag{B13}$$

Thus we see that the relativistic set of equations will have exactly the same mathematical form as $\lambda = 0$ version of (43)–(46); the only difference is that the Alfvén speed is modified due to a constant $\gamma_0$, $v_A^2 = B_0^2/4\pi\rho_0\gamma_0$. The structural equivalence proves that all the later results are valid for the relativistic weakly-sheared flows.

In this derivation ,we have still neglected the displacement current. This assumption is justified as long as $v_A/c \ll 1$. For a strongly magnetized, relativistic e-p plasma, however, the displacement current must be retained for a proper description. This will, indeed, be done in the forthcoming work.

## Acknowledgments

This work was supported by the U.S. Dept. of Energy Contract No. DE-FG03-96ER-54346.

ADR's research was supported, in part, by International Science Foundation (ISF) long-term research grant RVO 300. ADR's visit to ICTP was supported, in part, by the Committee for Science and Technology of Republic of Georgia. VIB's research was supported, in part, by International Science Foundation (ISF) long-term research grant KZ3200.

## References


1. P.A. Sturrock, Astrophys. J. **164**, 529 (1971); M.A. Ruderman and P.G. Sutherland, Astrophys. J. **196**, 51 (1975); J. Arons and E.T. Scharlemann, Astrophys. J. **231**, 854 (1979); J.K. Daugherty and A.K. Harding, Astrophys. J. **252**, 337 (1982); F.C. Michel, *Theory of Neutron Star Magnetospheres* (University of Chicago Press, Chicago 1991).

2. D.B. Melrose, J. Astrophys. Astr. **16**, 137 (1995).

3. M.C. Begelman, R.D. Blandford, and M.D. Rees, Rev. Mod. Phys. **56**, 255 (1984).

4. M.L. Burns, in *Positron–Electron Pairs in Astrophysics*, ed. M.L. Burns, A.K. Harding, and R. Ramaty (American Institute of Physics, New York, 1983).

5. K. Holcomb and T. Tajima, Phys. Rev. D **40**, 3809 (1989); T. Tajima and T. Taniuti, Phys. Rev. A **42**, 3587 (1990); V.I. Berezhiani and S.M. Mahajan, Phys. Rev. Lett. **73**, 1110 (1994); V.I. Berezhiani and S.M. Mahajan, Phys. Rev. E **52**, 1968 (1995).

6. C.M. Surko, M. Leventhal, and A. Passner, Phys. Rev. Lett. **62**, 901 (1989); R.G. Greaves, M.D. Tinkle, and C.M. Surko, Phys. Plasmas **1**, 1439 (1994).

7. G.A. Stewart and E.W. Laing, J. Plasma Phys. **47**, 295 (1992); N. Iwamoto, Phys. Rev. E **47**, 604 (1993).

8. G.P. Zank and R.G. Greaves, Phys. Rev. E **51**, 6079 (1995).

9. A.B. Mikhailovskii, O.G. Onishchenko, and E.G. Tatarinov, Plasma Phys. and Contr. Fusion **27**, 527 (1985).

10. A.D. Verga and C.F. Fontan, Plasma Phys. and Contr. Fusion **27**, 19 (1985).

11. W.O. Criminale and P.G. Drazin, Stud. Appl. Math. **83**, 123 (1990); L.N. Trefethen, A.E. Trefethen, S.C. Reddy, T.A. Driscoll, Science **261**, 578 (1993); G.D. Chagelishvili, R.G. Chanishvili, T.S. Hristov, and J.G. Lominadze, Phys. Rev. E **47**, 366 (1993); W.O. Criminale, T.L. Jackson, and J. Lasseigne, J. Fluid Mech. **294**, 283 (1995); R. Matsumoto and T. Tajima, Astrophys. J. **445**, 767 (1995).

12. G.D. Chagelishvili, A.D. Rogava, and I.N. Segal, Phys. Rev. E **50**, 4283 (1994).

13. G.D. Chagelishvili, A.D. Rogava, and D.G. Tsiklauri, "Magnetohydrodynamic Waves in Sheared Plasmas, Phys. Rev. E (submitted).

14. G.D. Chagelishvili and O.V. Chkhetiani, Pis'ma v JETF **62**, 294 (1995).

15. A.D. Rogava and S.M. Mahajan, "Coupling of sound with internal gravity waves in parallel shear flows," I.C.T.P. preprint (IC/95/388), submitted to Phys. Rev. E (1995).

16. A. Hasegawa and C. Uberoi, *"The Alfvén wave"* (Technical Information Center, U.S. Department of Energy, Springfield, 1982); M.Y. Yu, P.K. Shukla, and L. Stenflo, Astrophys. J. Lett. **309**, L63 (1986).

17. S.M. Mahajan, Phys. Scripta **T60**, 160 (1995).

18. G.M. Murphy, *Ordinary Differential Equations and Their Solutions*, (Van Nostrand Company, Princeton 1960); M. Abramowitz and I.A. Stegun *Handbook of Mathematical Functions*, (Dover, New York, 1972).

19. G.L. Kotkin and V.G. Serbo, *Collection of Problems in Classical Mechanics*, (Pergamon Press, New York, 1971).

20. V.L. Ginzburg and V.V. Zheleznyakov, Ann. Rev. Astron. Astrophys. **13**, 511 (1975); D.B. Melrose, *Instabilities in Space and Laboratory Plasmas* (Cambridge University Press, Cambridge 1986); D.B. Melrose, Ann. Rev. Astron. Astrophys. **29**, 31 (1991).

21. D.B. Melrose, Astrophys. J. **225**, 557 (1978); J. Arons and J.J. Barnard, Astrophys. J. **302**, 120 (1986); J.G. Lominadze, G.Z. Machabeli, G.I. Melikidze, and A.D. Pataraya, Sov. J. Plasma Phys. **12**, 712 (1986); A.Z. Kazbegi, G.Z. Machabeli, and G.I. Melikidze, Mon. Not. R. Astron. Soc. **253**, 377 (1991); Q. Luo, D.B. Melrose, and G.Z. Machabeli, Mon. Not. R. Astron. Soc. **268**, 159 (1994).

## FIGURE CAPTIONS

FIG. 1. $b_y(\tau)/b_y(0)$ [(a)] and $\mathcal{E}(\tau)/\mathcal{E}(0)$ [(b)] versus $\tau$ for 2-D ($\gamma = 0$) spatial Fourier harmonics (SFH), for an initial pure compressional Alfvén perturbation. Other parameters of the system are: $\beta_0 = 10$, $R = 0.1$, and $\epsilon = 0.5$. The solid line on Fig. 1(b) displays numerically calculated $\mathcal{E}(\tau)$, while the circles represent $\mathcal{E}(\tau)$ calculated by the approximate equation (73).

FIG. 2. $b_z(\tau)/b_z(0)$ [(a)] and $\mathcal{E}(\tau)/\mathcal{E}(0)$ [(b)] versus $\tau$ for 2-D ($\gamma = 0$) SFH for an initial pure shear Alfvén perturbation. Other parameters of the system are: $\beta_0 = 10$, $R = 0.1$, and $\epsilon = 0.5$. The solid line on Fig. 2(b) displays numerically calculated $\mathcal{E}(\tau)$, while the circles represent $\mathcal{E}(\tau)$ calculated by the approximate equation (73).

FIG. 3. The temporal evolution of 3-D SFH ($b_y(\tau)/b_y(0)$ [(a)] and $\mathcal{E}(\tau)/\mathcal{E}(0)$ [(b)]) for an initially pure shear Alfvén mode with $\beta_0 = 10$, $R = 0.1$, $\epsilon = 5 \times 10^{-3}$, and $\gamma = 0.1$;

FIG. 4. The temporal evolution of 3-D SFH ($b_y(\tau)/b_y(0)$ [(a)] and $\mathcal{E}(\tau)/\mathcal{E}(0)$ [(b)]) for an initially pure shear Alfvén mode with $\beta_0 = 10$, $R = 0.1$, $\epsilon = 5 \times 10^{-3}$, and $\gamma = 1$;

Figure 1 (a)

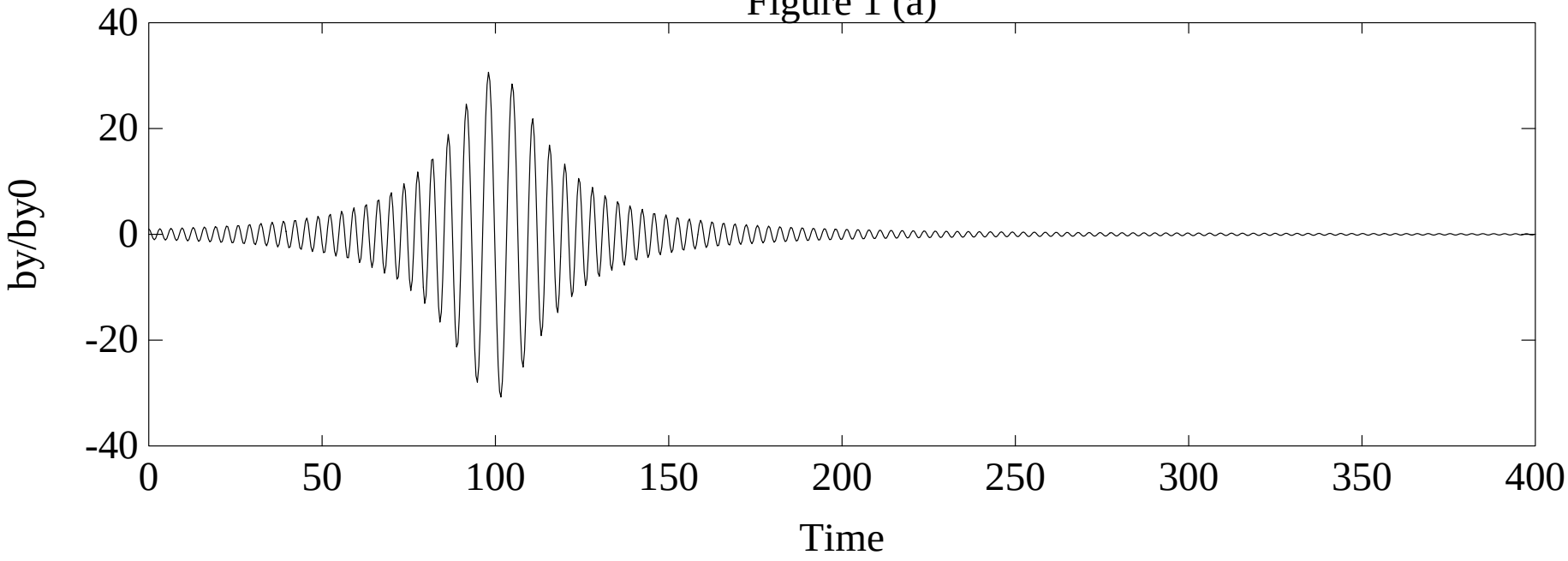


Figure 1 (b)

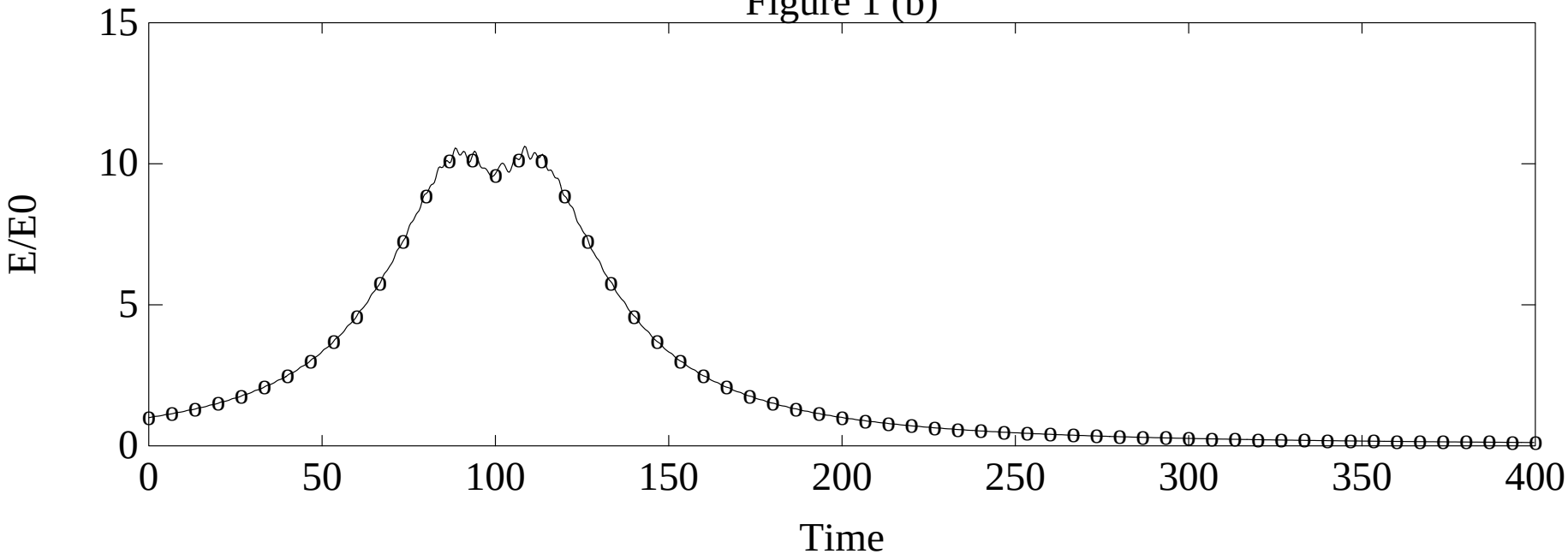

Figure 2 (a)

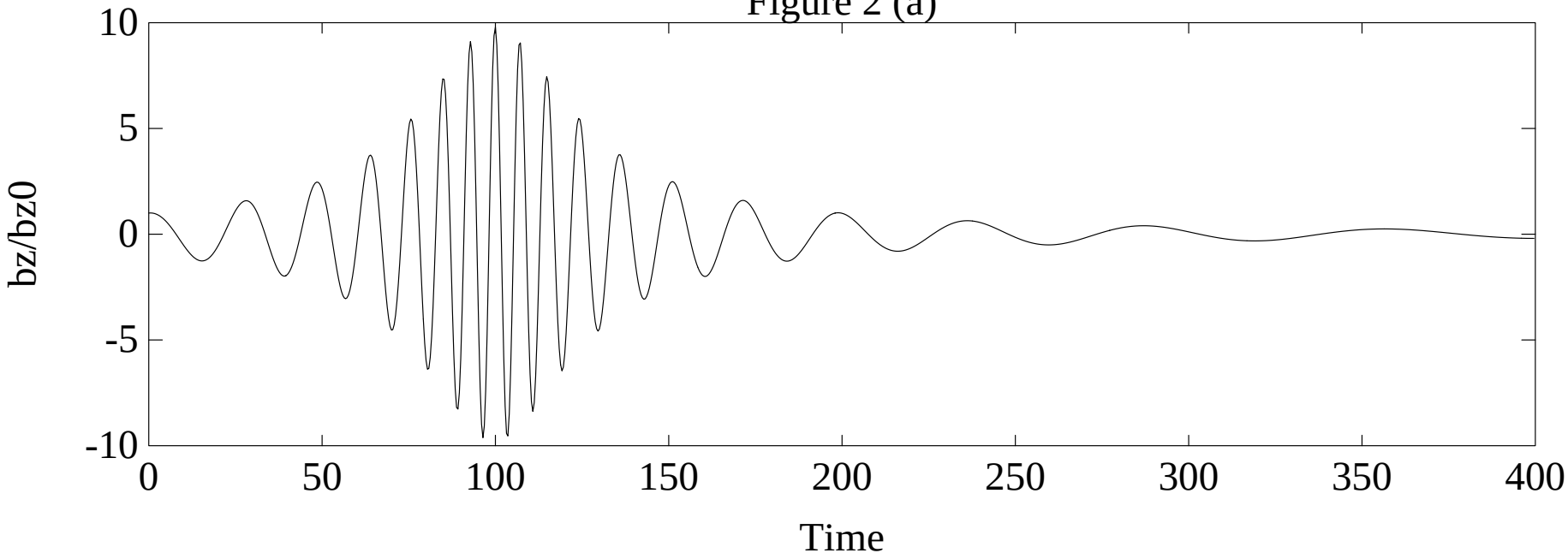


Figure 2 (b)

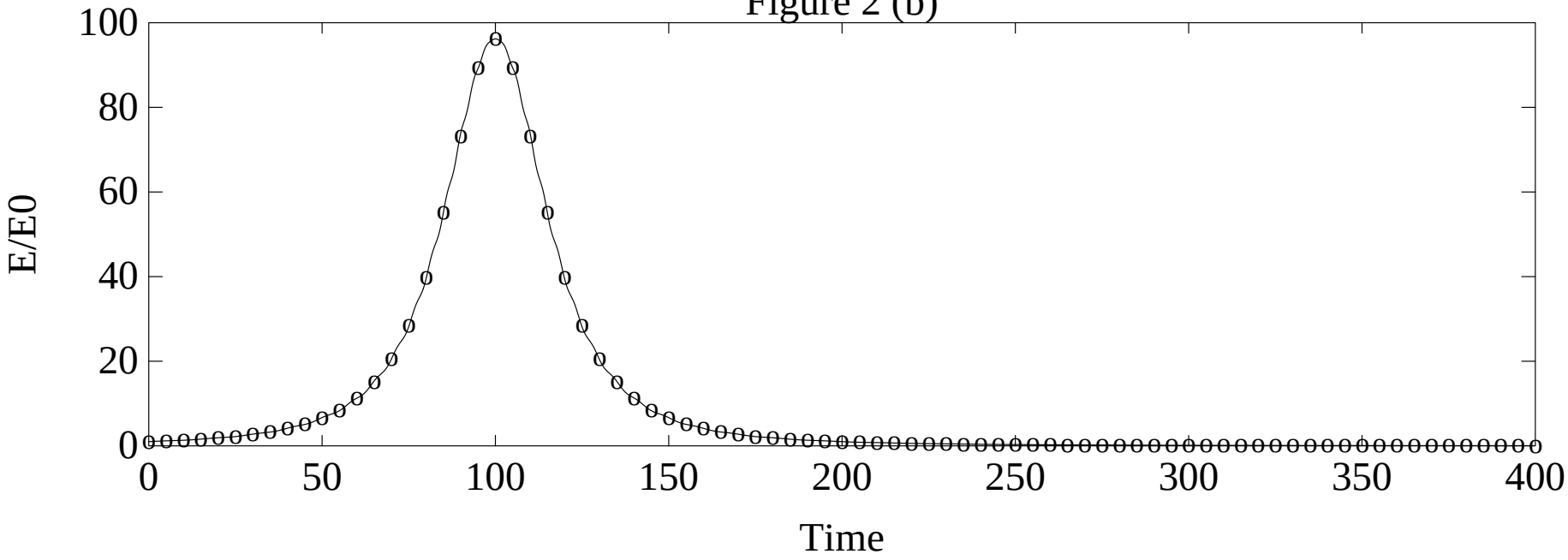

Figure 3 (a)

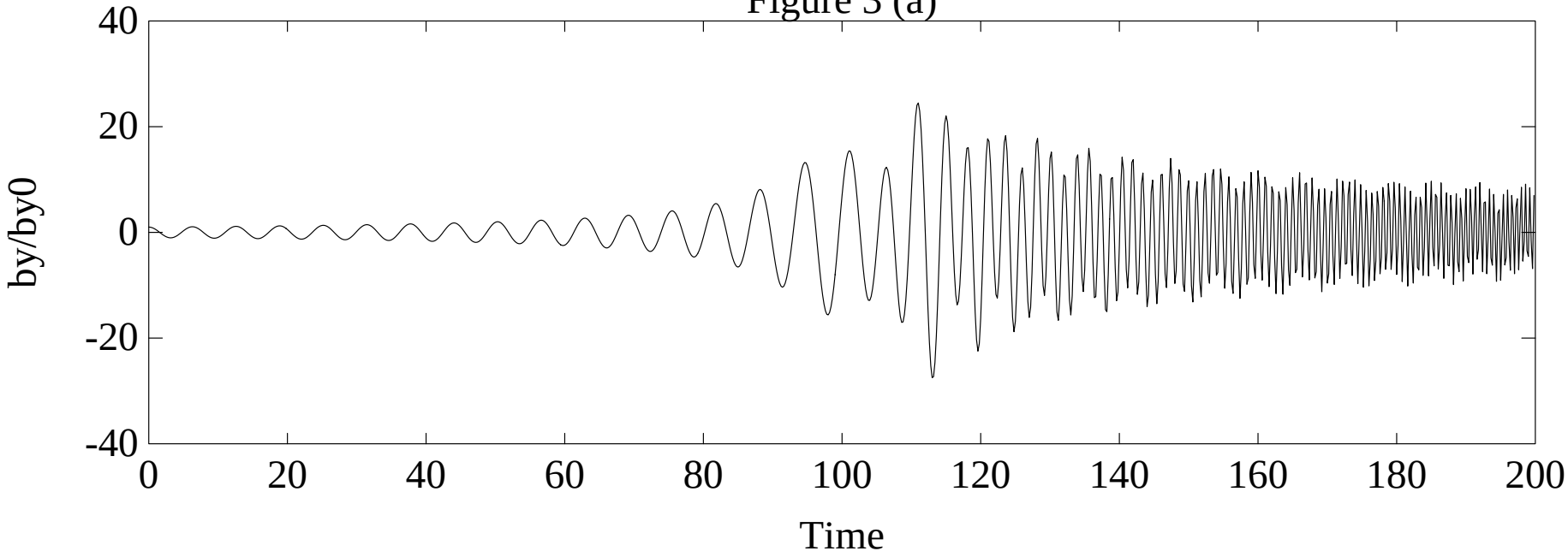


Figure 3 (b)

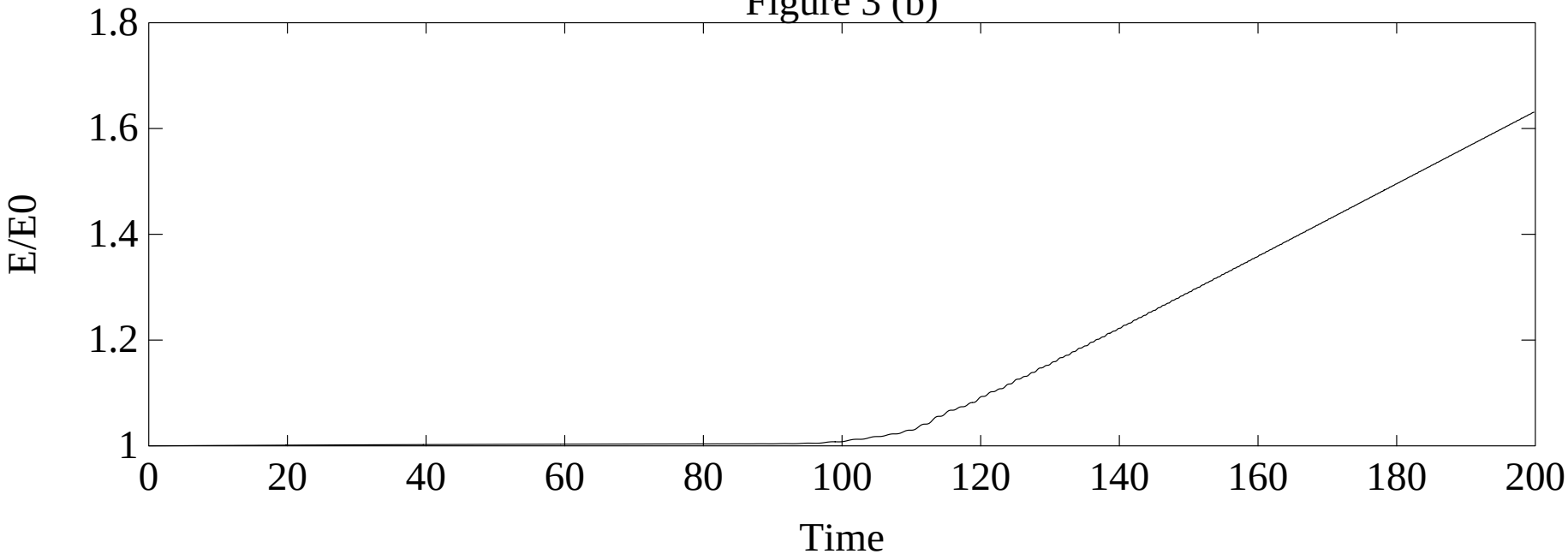

Figure 4 (a)

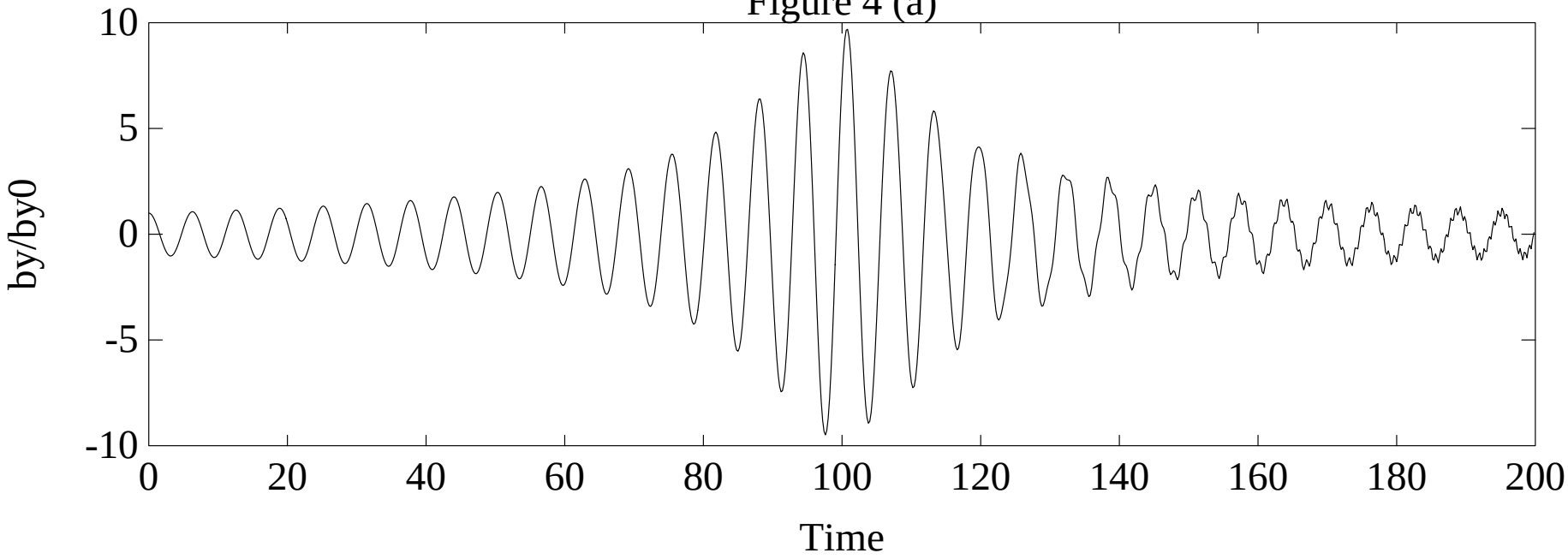


Figure 4 (b)